ROSAT/HRI study of the optically rich, lensing cluster CL0500-24

Sabine Schindler[1,2] **& Joachim Wambsganss**[3]

[1] MPI für extraterrestrische Physik, Giessenbachstr., 85748 Garching, Germany; e-mail: `sas@mpa-garching.mpg.de`
[2] MPI für Astrophysik, Karl-Schwarzschild-Str. 1, 85748 Garching, Germany
[3] Astrophysikalisches Institut Potsdam, An der Sternwarte 16, 14482 Potsdam, Germany; e-mail: `jwambsganss@aip.de`

arXiv:astro-ph/9607064v1 12 Jul 1996

Abstract. An analysis of a ROSAT/HRI observation of the optically rich, gravitationally lensing galaxy cluster CL0500-24 (or Abell S0506) is presented. We show that the X-ray luminosity of this supposedly rich cluster is relatively low at $1.1^{+0.2}_{-0.1} \times 10^{44}$ erg/s in the ROSAT band, the bolometric X-ray luminosity is $2.0^{+1.5}_{-0.7} \times 10^{44}$ erg/s. The X-ray emission is strongly correlated with the northern subconcentration of the cluster galaxies at redshift $z = 0.327$. The derived total mass of the (sub-)cluster within 1 Mpc is $(1.5 \pm 0.8) \times 10^{14} M_{\odot}$, with an upper limit to the gas mass of about $0.5 \times 10^{14} M_{\odot}$, corresponding to a gas mass fraction of $\leq 30^{+30}_{-10}\%$. The X-ray luminosity and the morphology of the extended X-ray emission supports the view that CL0500-24 consists of two clusters at a velocity difference of $\Delta v \approx 3200$ km/s that happen to lie along the line of sight.

Key words: Galaxies: clusters: individual: CL0500-24 – Galaxies: clusters: individual: Abell S0506 – intergalactic medium – Cosmology: observations – dark matter – X-rays: galaxies

1. Introduction

The cluster CL0500-24 is a medium redshift (z ≈ 0.32), rich cluster of galaxies (Giraud 1988). Optically there are two obvious subconcentrations visible (Infante et al. 1994). There is a straight blue arc in the cluster whose redshift ($z_{arc} = 0.913$) clearly identifies it as a background galaxy (Smail et al. 1993), thus confirming the gravitational lens scenario suggested by Wambsganss et al. (1989).

Since there has been some debate in the past whether the various mass determinations for clusters of galaxies – velocity dispersions, gravitational lens masses, X-ray masses – result in consistent or discrepant results (see

Send offprint requests to: Sabine Schindler

e.g. Miralda-Escudé & Babul 1995; Tyson & Fischer 1995; Smail et al. 1995; Squires et al. 1996a, 1996b), this cluster seems to be a good target for another test of these methods against each other.

X-ray observations of a galaxy clusters can provide information about the structure of clusters and therefore on their dynamical state. This is of interest here, since the optical appearance suggests physically distinct subclumps.

Here we present X-ray observations with the ROSAT/HRI (Trümper 1983). We show the morphology of CL0500-24 as it appears in X-rays, we determine an X-ray profile, and we estimate the mass of the X-ray emitting gas and the total mass of the cluster. Finally, we discuss our results and compare them with other X-ray/lensing clusters. Throughout this paper we use $H_0 = 50$km/s/Mpc.

2. The cluster CL0500-24 (or Abell S0506) in optical light

The cluster CL0500-24 is a rich, very compact southern cluster of galaxies (Giraud 1988) at a redshift of $z \approx 0.32$ (in Abell et al. (1989) it is listed as supplementary cluster S0506). There are 95-100 galaxies brighter than V = 23 within a radius of $\approx 0.55h_{50}^{-1}$Mpc. The average density, $N_{0.5}$, defined as the number of bright galaxies, $m \leq m_3 + 2$ (where m_3 is the magnitude of the third brightest galaxy) projected within a radius of $0.5h_{50}^{-1}$Mpc is 31-36. This means that CL0500-24 appears richer than the well studied giant gravitational arc cluster Abell 370, for which $N_{0.5} = 28$, see Mellier et al. (1988). CL0500-24 contains a large fraction of blue galaxies, and has a quite high line of sight velocity dispersion of $\sigma = 1375$km/s, based on redshifts of 22 cluster galaxies (Giraud 1990). The cluster "apparently has a triple core" (Giraud 1988) so it is to be expected that an X-ray map will identify substructure. Infante et al. (1994) also found a bimodal distribution in the galaxy velocities, enhancing this view that the cluster consists of subclumps.

The known redshifts of the galaxies in CL0500-24 cover quite a broad range. Infante et al. (1994) showed that the velocity distribution (26 measured galaxies) is bimodal with two peaks at $v_1 = 94817$ km/s and $v_2 = 97987$ km/s. The velocity difference ($\Delta v = v_2 - v_1 = 3170$ km/s) is much larger than the one-dimensional velocity dispersions of the two sub-clumps ($\sigma_1 = 917 \pm 208$ km/s, $\sigma_2 = 1152 \pm 214$ km/s). This double nature of the cluster was supported by Infante et al. (1994)'s group finding algorithms. So it appears that CL0500-24 is not one rich cluster, but rather two clusters along the line of sight.

The most striking feature in CL0500-24 is a straight, blue arc with a length of about 14 arcseconds, which is about 22 arcseconds away from the apparent cluster center. A gravitational lens model for this arc (Wambsganss et al. 1989) finds very naturally a strongly elongated image of a background galaxy at the position of the arc with the correct orientation. This model predicts a mass of about $1.4 \times 10^{14} M_\odot$ for the (projected) inner part of the cluster, i.e. for a circle around the apparent center C with radius center-arc (cf. Giraud 1990). Equivalently, a cluster modeled as a singular isothermal sphere with a velocity dispersion of 1430 km/s is necessary to produce an arc with this length at this location. The redshift of the arc was recently measured to be $z_{arc} = 0.913$ (see Smail et al. 1993) confirming the gravitational lens scenario quite satisfactorily. So far no arclets or weak lensing signature have been reported in this cluster.

3. X-ray Data

CL0500-24 was observed with the ROSAT/HRI in a pointed observation with an exposure time of 37756 s between February 8th and 13th, 1995.

The positioning of the observation can be checked with a point-like source which coincides with a star of blue magnitude 16.8 at a position $\alpha = 05^h01^m26.0^s$, $\delta = -24°17'31''$ (J2000). From this correspondence we infer that the positional accuracy of the pointing is very good (estimated error ≤ 4 arcseconds). The total number of source photons for the cluster CL0500-24 is 440.

As the cluster emission is not very strong we follow a two-fold strategy. In addition to the straightforward analysis of the full data set, we try to improve the signal-to-noise ratio by skipping the intervals with enhanced background. In practice, we bin the data to intervals of 100 s. Subsequently, we drop the high background intervals with more than 500 counts / 100 s. The remaining time intervals with the "cleaned data" cover 57% of the original exposure time. The cleaned data set contains 270 source photons.

3.1. Morphology

Because of the limited number of photons from the cluster the observed morphology is influenced by statistical fluc-tuations. In Fig. 1 we present an image smoothed with a Gaussian filter of $\sigma = 10$ arcseconds to give an idea how the morphology looks like. The main maximum of an image smoothed with a Gaussian of $\sigma = 5$ arcseconds is at $\alpha = 05^h01^m05.6^s$, $\delta = -24°25'03''$ (J2000). It corresponds to a position between the galaxies N and S (nomenclature according to Giraud (1990)) which are identified by Infante et al. (1994) as the center of one of two sub-concentrations. In an image smoothed with a Gaussian of $\sigma = 10$ arcseconds the X-ray maximum is also very close to these galaxies (see Fig. 2). The X-ray emission is elongated southward towards galaxy A. A second maximum of the X-ray emission can be seen in the North-East at $\alpha = 05^h01^m09^s$, $\delta = -24°24'31''$ (J2000), close to galaxy # 12 (cf. Infante et al. 1994). There is no extra emission associated with the second optical center C. All these features are "robust" in that they show up both in the "cleaned" and in the "non-cleaned" data.

The galaxies are assigned to two subclusters centred on galaxy N and on galaxy C, respectively, by Infante et al. (1994) according to their velocities from Giraud (1990) and Infante et al. (1994). The distribution of N galaxies is much better correlated with the X-ray emission than the distribution of C galaxies (see Fig. 2). This is a first hint that we see in X-rays only (or mainly) the N subcluster.

In Fig. 3 the X-ray morphology is compared with the galaxy density (Infante, private communication) for all galaxies, while in Fig. 2 only galaxies with measured velocities are included. The luminosity weighted densities show again the two main concentrations around N and C, out of which only N is correlated with X-rays. Another maximum in the galaxy density in the north-east is situated between two X-ray blobs and is probably belonging to the N concentration because there are three N galaxies in this region, i.e. again no indication for any emission from the C subcluster.

3.2. Luminosity

The X-ray emission can be traced out to a radius of 2.5 arcminutes (860 kpc at distance of cluster). As summarized in Table 1, we find a countrate of 0.012 ± 0.001 counts/s within this radius. To convert this countrate to a luminosity we assume a typical metallicity of 0.35 solar (Arnaud et al. 1992; Ohashi 1995) and a Galactic hydrogen column density of 7.12×10^{22} cm^{-2} (Dickey & Lockman 1990). As there is no possibility to derive a gas temperature with the HRI we assume a typical cluster temperature of 4 keV which is also consistent with the $L_X - T$ relation (Edge & Stewart 1991a; David et al. 1993; White 1996). With these values the luminosity in the ROSAT band (0.1 - 2.4 keV) is $1.1^{+0.2}_{-0.1} \times 10^{44}$ erg/s and the bolometric luminosity is $2.0^{+1.5}_{-0.7} \times 10^{44}$ erg/s. The errors include the uncertainties of the countrate and an assumed temperature range between 1 and 10 keV.
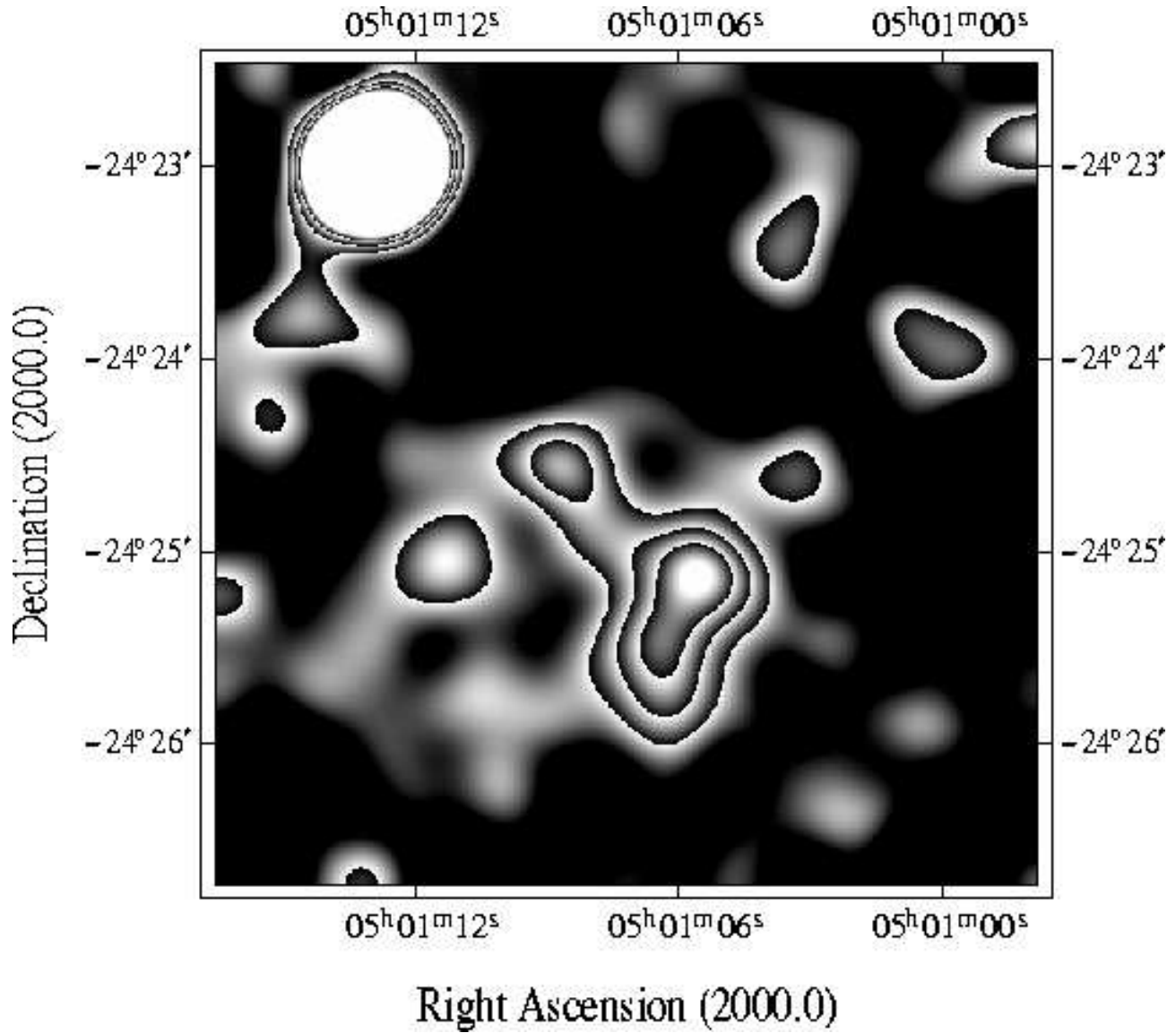
Fig. 1. ROSAT/HRI image of the cluster CL0500-24. It is smoothed with a Gaussian filter of $\sigma = 10$ arcseconds. The cluster has a clumpy structure with an extension south of the maximum and additional emission in the north-east and in the east. The bright X-ray source in the upper left corner is not associated with the cluster.

About 2.6 arcminutes north-east of the cluster centre is a point-like source (see Fig. 1) at $\alpha = 05^h01^m13^s$, $\delta = -24°22'59''$ (J2000). It has a countrate of 8.6×10^{-3} counts/s. The position of this source corresponds within 10 arcseconds to the radio source PMN0501-2422 which is listed in Griffith et al. (1994) with a 4850 MHz flux density of 154 mJy. Looking for an optical counterpart in the Southern Digitized Sky Survey we find a faint object at about 4 arcseconds distance; it cannot be distinguished whether it is a stellar object or a galaxy.

3.3. Profile

Because of the limited number of photons and the non-spherical appearance of the X-ray contours, the radial profile of the X-ray emission is not very well determined (Fig. 4). Nevertheless, we try to fit a β-model to the surface brightness (following Cavaliere & Fusco-Femiano 1976; Jones & Forman 1984)

$$\Sigma(r) = \Sigma_0 \left(1 + \left(\frac{r}{r_c}\right)^2\right)^{-3\beta+1/2}, \qquad (1)$$

where Σ_0 is the central surface brightness, r_c is the core radius, and β is the slope parameter. The best fit values averaged over a number of fits with or without "cleaning" and
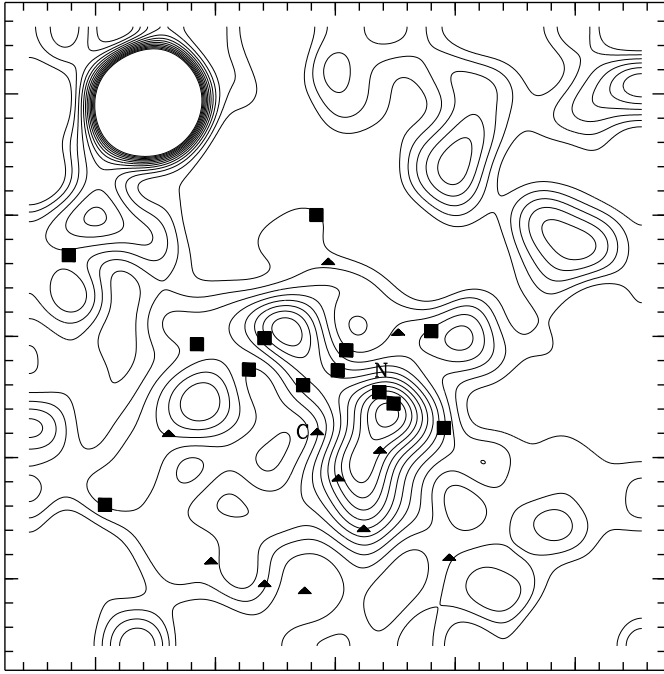
Fig. 2. Cluster galaxies assigned to the subclusters N and C by Infante et al. (1994) superimposed on the X-ray contours (smoothed with a Gaussian filter of $\sigma = 10$ arcseconds). Triangles: galaxies assigned to subcluster C, squares: galaxies assigned to subcluster N. The size of the image is the same as in Fig. 1. One tickmark corresponds to 10 arcseconds. The contour levels have a linear spacing of 3.8×10^{-4} counts/s/arcmin^2. The highest contour corresponds to 9.2×10^{-3} counts/s/arcmin^2, the lowest to 5.0×10^{-3} counts/s/arcmin^2. The central galaxies of the subclusters are marked with N and C, respectively. The X-ray emission is well correlated with the subcluster centred on N, while there is hardly any correlation with the C subcluster. In particular, there is no extra emission at the position of the central galaxy C.

with different binning centred on $\alpha = 05^h01^m05.6^s$ $\delta = -24°25'03''$ (J2000) are $\Sigma_0 = 8 \times 10^{-3}$ counts/s/arcmin^2, $r_c = 0.09$ arcminutes (30 kpc) and $\beta = 0.4$, a very small β and a very small core radius. But the 1σ errors allow for a huge range of about 0.3 to 1.0 for β and 0 to 1.5 arcminutes (0 to 500 kpc) for the core radius.

3.4. Mass determination

The parameters of the β-model can be used to make a deprojection of the 2D image to derive the three dimensional density distribution. The profile of the integrated gas mass is shown in Fig. 5. Within a radius of 1 Mpc the gas mass amounts to $0.46 \times 10^{14} M_\odot$. As the emissivity of the gas in the ROSAT energy band is almost independent of the temperature (within the temperature range of 2-10 keV it changes only by 6%), we can derive the gas density distribution hardly affected by the uncertainty of
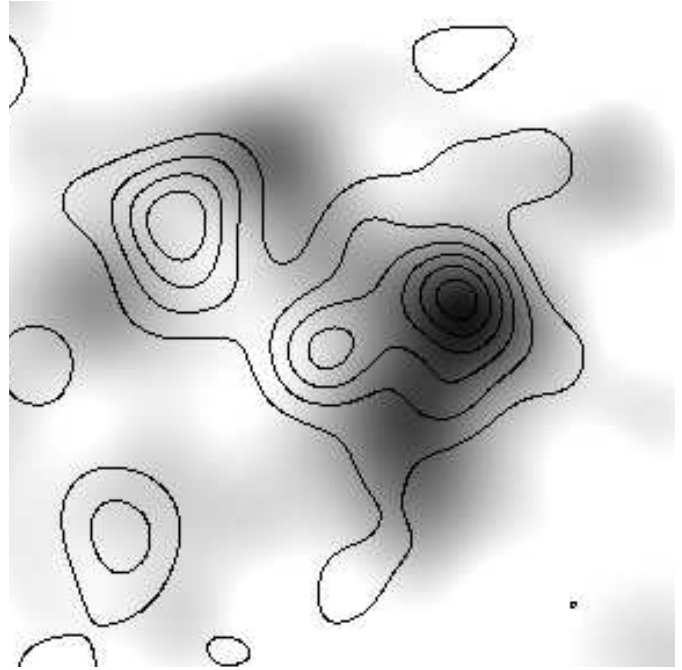

Fig. 3. Luminosity weighted galaxy densities (contours) from V magnitudes (Infante, private communication) smoothed with a Gaussian of $\sigma = 8$ arcseconds are superimposed on the X-ray emission (greyscales, same as the contours of Fig. 2). The size of the image is 2.5x2.5 arcminutes.
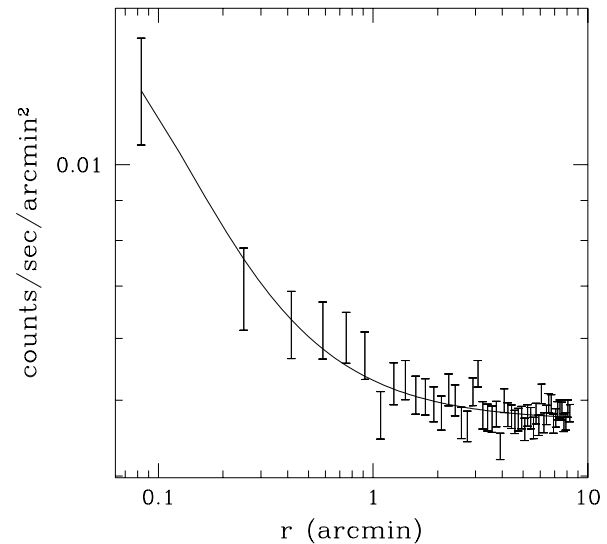

Fig. 4. Radial profile of the X-ray emission fitted with a β-model.

the temperature estimate. The only uncertainty are local unresolved inhomogeneities or substructure which result in an overestimation of the gas mass. Therefore, the value given above is strictly speaking an upper limit.

With the additional assumption of hydrostatic equilibrium, the integrated total mass can be calculated from the equation

$$M(r) = \frac{-kr}{\mu m_p G} T \left(\frac{d \ln \rho}{d \ln r} + \frac{d \ln T}{d \ln r} \right), \qquad (2)$$

where ρ and T are the density and the temperature of the intra-cluster gas, and r, k, μ, m_p, and G are the radius, the Boltzmann constant, the molecular weight, the proton mass, and the gravitational constant, respectively. For the temperature we use again a typical cluster temperature of 4 keV. When using the parameters of the various β-model fits with varying binning and with/out "cleaning" we find different mass profiles only in the central part, as shown in the section above. Beyond a radius of about 100 kpc the various mass profiles are in good agreement. The error originating from the uncertainty in the temperature is certainly much larger and can amount to $\pm 50\%$.

The results are shown in Fig. 5. At a radius of 1 Mpc we find an integrated total mass of $(1.5 \pm 0.8) \times 10^{14} M_\odot$. The errors comprise a temperature range from 2 to 6 keV. This total mass yields a relatively high gas mass fraction of $30^{+30}_{-10}\%$. The gas mass fraction is decreasing when going to smaller radii. But as the gas mass fraction depends on β and β is not very well defined (see Sect. 3.3) this decrease may not be very significant.

The total mass is even smaller than the luminosity-weighted virial mass of $2.2 \times 10^{14} M_\odot$ of only the N concentration derived by Infante et al. (1994). (The X-ray mass converted to their $H_0 = 60 \mathrm{km/s/Mpc}$ would be $1.3 \times 10^{14} M_\odot$.) This is a hint that the X-ray emitting gas traces the potential of only one subcluster.

For a comparison with mass estimates determined from the gravitational lensing effect, we also calculate the total mass of the cluster, as seen inside a certain angle, basically integrating a spherically symmetric three dimensional mass distribution in cylindrical shells with cylinder axis parallel to the line of sight or integrating the cluster surface mass density $\Sigma(\theta)$ outward (see Fig. 5). The total mass inside a circle with radius cluster center-arc is $0.3 \times 10^{14} M_\odot$. From the point lens model, Wambsganss et al. (1989) found a much larger value: $1.4 \times 10^{14} M_\odot$ (or a velocity dispersion of $\sigma = 1197$ km/s for an isothermal sphere model); here we used the now measured arc redshift of $z_{arc} = 0.913$ (Smail et al. 1993). Obviously, the mass from the lens model is considerably higher than the mass obtained here when integrating outward the total mass derived from the X-ray emission. But the two mass estimates are not directly comparable because the X-ray mass is centred on galaxy N while the lensing model has an assumed centre close to 'C'. There is a difference in these two mass determinations, but not a striking one.

However, this is not too surprising: the gravitational lens effect integrates all matter along the sight, and we just pointed out that there are *two* clusters along the line of sight. On the other hand, the X-ray mass determination is most sensitive to the highest density regions in the center of the cluster. Furthermore, the point lens or spherically symmetric isothermal sphere model used for the gravitational lens model (Wambsganss et al. 1989) is certainly too simple to account in detail for the action of two sub-concentrations along the line of sight.
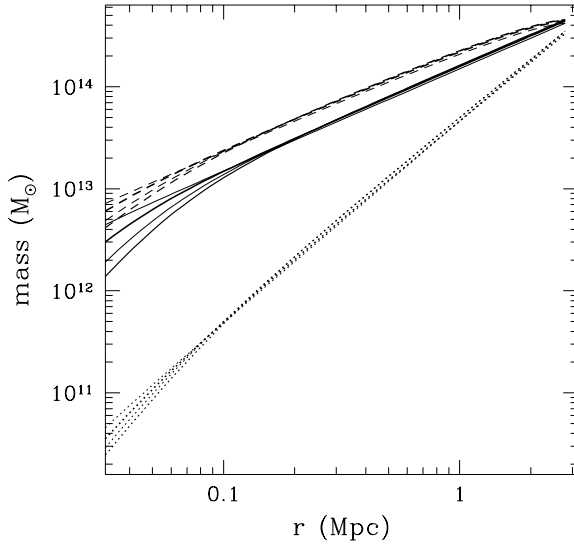

Fig. 5. Mass profile of Cl0500-24. The dotted lines show the integrated gas mass, the solid lines the integrated total mass. Profiles for data with/out "cleaning" and with different binning are plotted. In the inner region the scatter is quite large because of the limited number of photons. But beyond a radius of 100 kpc the profiles agree well. For comparison with mass determinations by the gravitational lens effect, the dashed lines depict the integrated surface mass density.

4. Discussion and conclusions

The X-ray luminosity of CL0500-24 is quite moderate. Actually, it is very small for a "rich" cluster of galaxies. The Abell Cluster A370 (at a comparable redshift), which supposedly is about equally rich as CL0500-24, is roughly ten times more luminous in X-rays (Lea & Henry 1988; Fabricant et al. 1991; Bautz et al. 1994). Does this show that there is a wide spread of X-ray luminosities for clusters that appear similarly rich optically?

countrate(0.1-2.4keV)	0.012 ± 0.001 counts/s
L_X(0.1-2.4keV)	$1.1^{+0.2}_{-0.1} \times 10^{44}$ erg/s
L_X(bol)	$2.0^{+1.5}_{-0.7} \times 10^{44}$ erg/s
$M_{gas}(r < 1\mathrm{Mpc})$	$0.5 \times 10^{14} M_\odot$
$M_{tot}(r < 1\mathrm{Mpc})$	$1.5 \pm 0.8 \times 10^{14} M_\odot$
gas mass fraction (< 1Mpc)	$30^{+30}_{-10}\%$

Table 1. Summary of the X-ray properties of CL0500-24

We argued that the X-ray emission of CL0500-24 originates mainly from the northern subclump. But even when comparing the bolometric luminosity of CL0500-24 only with the velocity dispersion of the Northern subcluster, it is unexpectedly low (Edge & Stewart 1991b). This indicates at least a moderate spread in the optical richness versus X-ray luminosity relation.

There are other examples that illustrate this, e.g. the two distant clusters CL0939+4713 and CL0016+16, which are both optically very rich (Dressler 1994; Koo 1981) but have quite different bolometric X-ray luminosities: 1.1×10^{45} erg/s (Schindler & Wambsganss 1996) and 5.6×10^{45} erg/s (Neumann & Böhringer 1996), respectively.

Given the bimodal velocity distribution of the galaxies in CL0500-24 (cf. Chapter 2), there are two possibilities for the spatial distance of the subclusters in the line of sight. One possible scenario is that the two subclusters are relatively unrelated and the different velocities are caused mainly by the Hubble flow. In this case they have a distance of more than 60 Mpc. The other possibility is that the two subclusters have a physical distance that is smaller than that corresponding to the redshift difference, and are in the process of colliding. As the relative velocity of almost 3200 km/s is very high, in such a scenario the subclusters would have to pass right through each other along the line of sight. In fact, the projected distributions of the galaxies with redshift z_2 preferentially north, and with z_1 preferentially south indicates, that such a collision could not be exactly along the line of sight, but with some angle relative to it. So the velocity difference is only the contribution projected onto the line of sight, and the real 3dim relative velocity must be even larger than the measured difference. N-body models show that relative velocities around 3000 km/s or more are reached only during a very short period of time as the subclusters pass through each other (Schindler & Böhringer 1993; Huss et al. 1996). If the subclusters are just passing through each other, an X-ray emission enhanced by a about a factor

of two relative to a quiescent state is expected during a collision (Schindler & Müller 1993). However, given the low observed X-ray luminosity, and the fact that it is very unlikely that we see CL0500-24 exactly in this extreme short phase corresponding to such an encounter with high relative velocity we conclude that it is extremely unlikely that the two subclumps are currently undergoing such a collision.

This view of two unrelated clusters is supported both by the morphology and the luminosity of the X-ray emission of the cluster. The X-rays originate from regions that are related to the subclump around N with galaxy velocities peaking at v_2. There is no significant detection from the supposed center of the cluster near the galaxy C (cf. Giraud 1990) or other galaxies at redshift z_1.

The mass assigned by Infante et al. (1994) to the more massive subclump around N at z_2 is even higher than the X-ray mass determined here. That is an indication that the X-rays trace the potential of only one subcluster while the southern subcluster around galaxy C apparently does not affect the X-ray mass determination. The mass found by Wambsganss et al. (1989) for the cluster from a simple gravitational lens model for the straight arc is higher than the X-ray mass determined here. This also fits into this picture qualitatively, because the gravitational lens effect integrates all the mass along the line of sight, and so unavoidably considers all the subclumps discussed here.

The total mass of $(1.5 \pm 0.8) \times 10^{14} M_\odot$ within 1 Mpc which is about the virial radius according to the spherical collapse approximation (Gunn & Gott 1972; White et al. 1993) is a relatively low value compared to the typical mass range of clusters of $5-50 \times 10^{14} M_\odot$ (Böhringer 1995). It is an order of magnitude lower than the mass of the nearby clusters Coma and Perseus (Böhringer 1994). The gas mass fraction of 30% is at the upper limit of the typical range for clusters of 10-30% (Böhringer 1995).

Combined, all the arguments mentioned above point into the direction that CL0500-24 consists of two concentrations with little direct interaction. Only one of the subclusters has X-ray emission. But even considering the fact that only part of the optically visible cluster is associated with the X-ray properties, the values for the X-luminosity and the derived total mass are comparably small.

References

Abell G., Corwin Jr. H.G., Olowin R.P., 1989, ApJS 70, 1
Arnaud M., Rothenflug R., Boulade O., Vigroux L., Vangioni-Flam E., 1992, A&A 254, 49
Bautz M.W., Mushotzky R., Fabian A.C., Yamashita K., Gendreau K.C., Arnaud K.A., Crew G.B., Tawara Y., 1994, PASJ 46, L131

Böhringer H., 1994, in: X-Ray Clusters of Galaxies, NATO Advanced Science Institute Vol. 441, Seitter, W.C. (ed.) Kluwer, Dordrecht, p. 123

Böhringer H., 1995, in: Proceedings of the 17th Texas Symposium on Relativistic Astrophysics and Cosmology, Böhringer H., Morfill G.E., Trümper J.E. (eds.), New York Academy of Sciences, New York, p. 67

Cavaliere A., Fusco-Femiano R., 1976, A&A 49, 137

David L.P., Slyz A., Jones C., Forman W., Vrtilek S.D., Arnaud K.A., 1993, ApJ 412, 479

Dickey J.M., Lockman F.J., 1990, ARA&A 28, 215

Dressler A., Oemler A., Butcher H.R., Gunn J.E., 1994, ApJ 430, 107

Edge A.C., Stewart G.C., 1991a, MNRAS 252, 414

Edge A.C., Stewart G.C., 1991b, MNRAS 252, 428

Fabricant D.G, McClintock J.E., Bautz M.W., 1991, ApJ 381, 33

Giraud E., 1988, ApJ 334, L69

Giraud E., 1990, A&AS 83, 1

Griffith M.R., Wright A.E., Burke B.F., Ekers R.D., 1994, ApJS 90, 179

Gunn J.E., Gott J.R., 1972, ApJ 176, 1

Huss A., Steinmetz M., Jain B., 1996, in preparation

Infante L., Fouqué P., Hertling G., Way M.J., Giraud E., Quintana H., 1994, A&A 289, 381

Jones C., Forman W., 1984, AJ 276, 38

Koo D.C., 1981, ApJ 251, L75

Lea S.M., Henry J.P., 1988, ApJ 332, 81

Miralda-Escudé J., Babul A., 1995, ApJ 449, 18

Mellier Y., Soucail G., Fort B., Mathez G., 1988, A&A 199, 13

Neumann D.M., Böhringer H., 1996, MNRAS, submitted

Ohashi T., 1995, in: Seventeenth Texas Symposium on Relativistic Astrophysics and Cosmology, Böhringer H., Morfill G.E., Trümper J.E. (eds.), New York Academy of Sciences, New York, p. 217

Schindler S., Böhringer H., 1993, A&A 269, 83

Schindler S., Müller E., 1993, A&A 272, 137

Schindler S., Wambsganss J., 1996, A&A, in press

Smail I., Ellis R., Aragon-Salamanca A., Soucail G., Mellier Y., Giraud E., 1993, MNRAS 263, 628

Smail I., Ellis R.S., Fitchett M.J., Edge A.C., 1995, MNRAS 273, 277

Squires G., Kaiser N., Babul A., Fahlman G., Woods D., Neumann D.M., Böhringer H., 1996a, ApJ 461, 572

Squires G., Neumann D.M., Kaiser N., Arnaud M., Babul A., Böhringer H., Fahlman G., Woods D., 1996b, ApJ submitted

Trümper J., 1983, Adv. Space Res. 2, 142

Tyson J.A., Fischer P., 1995, ApJ 446, L55

Wambsganss J., Giraud E., Schneider P., Weiss A., 1989, ApJ 337, L73

White D.A., 1996, in: Röntgenstrahlung from the Universe, Zimmermann H.U., Trümper J.E., Yorke H., MPE report 263, p. 621

White S.D.M., Efstathiou G., Frenk C.S., 1993, MNRAS 262, 1023